Cross-Site Reliability of Human Induced Pluripotent stem cell-derived Cardiomyocyte Based Safety Assays Using Microelectrode Arrays: Results from a Blinded CiPA Pilot Study

Daniel Millard,[*] Qianyu Dang,[†] Hong Shi,[‡] Xiaou Zhang,[§] Chris Strock,[¶] Udo Kraushaar,[‖] Haoyu Zeng,[‖‖] Paul Levesque,[‡] Hua-Rong Lu,[‖‖‖] Jean-Michel Guillon,[#] Joseph C. Wu,[**] Yingxin Li,[**] Greg Luerman,[††] Blake Anson,[a] Liang Guo,[a,b] Mike Clements,[*] Yama A. Abassi,[§] James Ross,[*] Jennifer Pierson,[c,1] and Gary Gintant[d]

[*]Axion Biosystems Inc, Atlanta, Georgia 30309; [†]US Food and Drug Administration, Center for Drug Evaluation and Research, Silver Spring, Maryland 20993; [‡]Bristol-Myers Squibb Company, Princeton, New Jersey 08543; [§]Acea Biosciences, San Diego, California 92121; [¶]Cyprotex, Watertown, Massachusetts 01746; [‖]Naturwissenschaftliches und Medizinisches Institut, Reutlingen, Germany; [‖‖]Merck & Co., Inc., Safety & Exploratory Pharmacology Department, West Point, Pennsylvania; [‖‖‖]Janssen, Beerse, Belgium; [#]Sanofi R&D Preclinical Safety, Paris, France; [**]Stanford University School of Medicine, Stanford Cardiovascular Institute, Stanford, California; [††]Ncardia, Leiden, The Netherlands; [a]Cellular Dynamics International a FujiFilm, Company, Madison, Wisconsin 53508; [b]Frederick National Laboratory for Cancer Research, Leidos Biomedical Research Inc, Frederick, Maryland 21702; [c]ILSI-Health and Environmental Sciences Institute, Washington, District of Columbia 20009; and [d]Integrative Pharmacology (Dept ZR13), Integrated Science and Technology. AbbVie, North Chicago, Illinois 60064

[1]To whom correspondence should be addressed at HESI, 740 15th St, NW, Suite 600, Washington, DC 20005. Fax: 202-659-3859; E-mail: jpierson@hesiglobal.org.

ABSTRACT

Recent *in vitro* cardiac safety studies demonstrate the ability of human induced pluripotent stem cell-derived cardiomyocytes (hiPSC-CMs) to detect electrophysiologic effects of drugs. However, variability contributed by unique approaches, procedures, cell lines, and reagents across laboratories makes comparisons of results difficult, leading to uncertainty about the role of hiPSC-CMs in defining proarrhythmic risk in drug discovery and regulatory submissions. A blinded pilot study was conducted to evaluate the electrophysiologic effects of 8 well-characterized drugs on 4 cardiomyocyte lines using a standardized protocol across 3 microelectrode array platforms (18 individual studies). Drugs were selected to define assay sensitivity of prominent repolarizing currents (E-4031 for I_{Kr}, JNJ303 for I_{Ks}) and depolarizing currents (nifedipine for I_{CaL}, mexiletine for I_{Na}) as well as drugs affecting multichannel block (flecainide, moxifloxacin, quinidine, and ranolazine). Inclusion criteria for final analysis was based on demonstrated sensitivity to I_{Kr} block (20% prolongation with E-4031) and L-type calcium current block (20% shortening with nifedipine). Despite differences in baseline characteristics across

cardiomyocyte lines, multiple sites, and instrument platforms, 10 of 18 studies demonstrated adequate sensitivity to I_{Kr} block with E-4031 and I_{CaL} block with nifedipine for inclusion in the final analysis. Concentration-dependent effects on repolarization were observed with this qualified data set consistent with known ionic mechanisms of single and multichannel blocking drugs. hiPSC-CMs can detect repolarization effects elicited by single and multichannel blocking drugs after defining pharmacologic sensitivity to I_{Kr} and I_{CaL} block, supporting further validation efforts using hiPSC-CMs for cardiac safety studies.

Key words: stem cell-derived cardiomyocytes; microelectrode array; cardiac electrophysiology; cardiac safety.

Drug-induced delayed ventricular prolongation is directly linked to a propensity of *Torsade de Pointes* (TdP), a rare but potentially lethal arrhythmia that remains of great concern to pharmaceutical and regulatory agencies. Current guidelines on the nonclinical evaluation of the proarrhythmic liability of drugs remain largely focused on *in vitro* studies of block of the potassium channel encoded by the human ether-à-go-go related gene (*hERG*) associated with QT prolongation, along with the direct assessment of QT prolongation in animal studies. These assays, along with clinical Through-QT (TQT) studies have been highly effective in preventing torsadogenic drugs from entering the market (eg, no drug withdrawals for proarrhythmia since ICH S7B and E14 guidelines). However, these nonclinical approaches may lack specificity, potentially leading to incorrect attribution of risk, unacceptable attrition of promising drug candidates, and the premature discontinuation of potentially useful (and, in some cases, life-saving) pharmaceuticals. It is now well recognized that block of the outward (repolarizing) *hERG* channel may be offset by concomitant block of inward (depolarizing) ion currents such as calcium or late sodium current mitigating any QT prolonging effects. Such is the case for drugs like verapamil and ranolazine, which reduce I_{Kr} without eliciting QT prolongation or risk of TdP in humans (Johannesen *et al.*, 2014; Kramer *et al.*, 2013). These findings suggest the need for a more comprehensive approach for nonclinical *in vitro* studies involving the integrated response to multiple ionic currents. Human induced pluripotent stem cell-derived cardiomyocytes (hiPSC-CMs) express multiple cardiac currents and exhibit an electrophysiologic phenotype comparable, though not identical, to native adult ventricular myocytes (Ma *et al.*, 2011; van den Heuvel *et al.*, 2014), and may define proarrhythmic risk with equivalent sensitivity and higher specificity than previous single ionic current model approaches. However, blinded multisite validation studies are needed to confirm their utility and practical limitations of these assays.

The Comprehensive *in vitro* Proarrhythmia Assay (CiPA), initiated by the US Food and Drug Administration (FDA), aims to redefine the nonclinical evaluation of TdP liability (Gintant *et al.*, 2016; Sager *et al.*, 2014) with an integrated, mechanistic-based assessment of proarrhythmic risk. Specifically, the CiPA paradigm will define a proarrhythmia risk ranking using a multifaceted approach that combines: (1) *in silico* models providing reconstructions of the drug effects on ventricular electrophysiologic activity based on measured effects on individual human cardiac ionic currents, (2) direct *in vitro* evaluations of integrated electrophysiologic responses with human stem cell-derived cardiomyocytes, and (3) carefully designed ECG-based first-in-human Phase 1 clinical trials (Sager *et al.*, 2014).

Microelectrode array (MEA) technology has been used for decades to study the electrophysiology of neurons and cardiomyocytes (Meiry *et al.*, 2001; Reppel *et al.*, 2004; Thomas *et al.*, 1972). For assessing cardiomyocyte electrophysiology,

electrodes embedded in a cell culture substrate noninvasively interface with established and interconnected cardiomyocytes, simultaneously providing functional measures of electrical activity across wells and without perturbing the cellular network. The electrophysiological signal obtained from the surface mounted microelectrodes (termed field potentials) arises from the cardiac action potential that propagates across the electrode array, providing measures of depolarization and repolarization phases of the cardiomyocytes related to corresponding measures from the cardiac action potential waveform (Asai *et al.*, 2010; Asakura *et al.*, 2015). Recent studies demonstrate the utility of human stem cell-derived cardiomyocytes and MEA assays for the *in vitro* evaluation of electrophysiologically based cardiac safety liabilities (Blinova *et al.*, 2017; Braam *et al.*, 2010; Clements and Thomas, 2014; Harris *et al.*, 2013; Kitaguchi *et al.*, 2016; Nakamura *et al.*, 2014; Navarrete *et al.*, 2013).

Here, we describe results from the CiPA MEA Pilot Study, coordinated by the Health and Environmental Sciences Institute (HESI), that compared the functional concentration-dependent electrophysiologic effects of 8 blinded, well-characterized drugs in 18 studies across 4 cardiomyocyte types, 3 MEA platforms, and 13 performance sites. The goal of this pilot study was to evaluate the utility and consistency of results from hiPSC-CMs on MEA-based platforms using a standardized protocol across multiple myocyte types and experimental sites. To minimize variability across sites, a common core protocol was developed that defined cell preparations, experimental protocol, and analysis measurements while retaining flexibility to accommodate variations across cell lines and experimental platforms. Inclusion criteria were established based on pharmacologic sensitivity to 2 prominent currents that define repolarization, namely outward (I_{Kr}) and inward (I_{CaL}) current. For the 10 of 18 studies satisfying the inclusion criteria, reproducible concentration-dependent electrophysiologic responses were observed that were consistent with known electrophysiologic mechanisms. These results support further validation studies of the hiPSC-CM-MEA assay within the CiPA paradigm.

METHODS

CiPA core protocol. In an effort to evaluate reproducibility across sites, a standardized core protocol was developed that defined the cell preparation methods, experimental protocol, and analysis measurements. This core protocol retained flexibility to accommodate variations across the cell and platform combinations in the study. The common elements of the core protocol are described here and summarized in Table 1, along with any deviations noted.

Cell culture. Human stem cell-derived cardiomyocytes provided by 4 suppliers (Cellular Dynamics International [CDI],

Table 1. CM-MEA Assay Core Protocol for the CiPA Pilot Study

Protocol	Recommendation	Deviations
Compound concentration	10x for 10% media addition/withdrawal	
Compound prep date	Prepared day of dosing	
Cmpd plate conditions	37°C, 5% CO_2; Plate warmed during dosing	
Media for compound prep	Cell source recommendation	
Well replicates	$n = 3$ replicates per concentration	
Environmental control	37°C, 5% CO_2	
Dosing method	Single dose per well	
Baseline recording	2 min collected after 25–30 min equilibration	
Postdose recording	2 min collected 25–30 min postdose	2 min collected 55–60 min postdose (N=1)
Time-matched vehicle controls	3 wells/plate	1 well/plate for 6 and 9 well platforms (N=7)
Minimum reported endpoints	FPD, BP, SA, EAD occurrence	

The protocol specified key conditions for culture preparation and experiment execution. Deviations refer to known changes in experimental protocol, with the number of sites indicated.

Axiogenesis [AXG], GE Healthcare [GEH], and Stanford Cardiovascular Institute [SCI]) were plated according to cell supplier recommendations for specific cell-platform combinations. Supplier specifications included surface coating procedures, cell density, media composition, and volume per well, and time in culture required to mature cells prior to dosing. Protocols were designed to achieve an interconnected syncytium of cardiomyocytes, referred to elsewhere in the manuscript as simply cardiomyocytes. The origins and characteristics of the various cell types have been described previously in the literature (Clements and Thomas, 2014; Ma *et al.*, 2011; Navarrete *et al.*, 2013). In all cases, the media was changed at least 2 h prior to the experiment to allow cell culture equilibration.

Experimental protocol. On the day of the experiment, the cell culture plate was moved directly from the incubator to the MEA device for baseline recordings. Environmental controls (37°C and 5% CO_2) were used to maintain the temperature and pH.

A single dosing scheme was utilized, such that each culture well received only one concentration of a particular compound, with a replicate set of 3 wells for each concentration. Compounds were prepared fresh daily at 10x the final concentration in maintenance media and stored in an incubator at 37°C and 5% CO_2 until added to test wells. Drugs were added to test wells by removing 10% of the media volume and replacing with the same volume of the prepared compound. In some cases, dosing was performed while the plate remained on the MEA device to minimize mechanical and temperature perturbations. Otherwise, the drug was added in a biosafety cabinet, returned to the MEA device, and environmental controls reengaged. In each case, the time required to dose the plate (under 10 min in all studies) was noted by the investigator. Baseline and postdose recordings were at least 2 min in length, with the postdose recording occurring 25 min after drug administration (to allow for drug equilibration). This time point was chosen to represent the acute electrophysiologic response that is the focus of the CiPA intitiative. Vehicle (0.1% DMSO) controls were included on each multiwell plate. Vehicle controls were run in parallel MEA chips for the single-chip MCS platform due to space limitations on the six or nine well MCS chips.

MEA platforms and data analysis. Three MEA platforms were utilized: the Maestro multiwell electrophysiology platform (Axion BioSystems, Inc. [AXN]), the MEA2100 system (Multi Channel Systems GmbH [MCS]), and the CardioECR system (ACEA Biosciences [ACA]). Analysis software specific to each instrument was used to provide 4 primary endpoints from the cardiac field potentials recorded: (1) spike amplitude (AMP), (2) field potential duration (FPD), (3) beat period (BP), and (4) arrhythmia occurrence (Figure 1). The onset of cardiac depolarization is marked by a sharp deflection in the field potential signal, termed the depolarization spike. The spike amplitude (AMP) provides an indirect measure of drug effects on the propagating action potential upstroke. Effects on cardiomyocyte repolarization are indicated by the repolarization features of the field potential. The field potential duration (FPD, roughly analogous to the QT interval of clinical ECGs) is defined by the interval between the depolarization spike and the peak of the repolarization feature. The BP was defined as the interval between 2 consecutive depolarization spikes. All endpoints were measured during a blinded analysis phase and submitted to a central resource for compilation across sites.

Depending on the platform, the above endpoints were derived from either a prescribed number of beats or a minimum time interval. In each case, the baseline and dosed measurements were taken during the final 5 min of a 30-min equilibration period (1 site used 60 min) on the MEA instrument (Figure 1A) to ensure proper environmental control, eliminate mechanical perturbations, and allow for the pharmacology to reach (near) equilibrium. For studies that recorded 2 min of data, the measurements were derived for each beat and averaged to generate a mean value. In studies that recorded continuously for the 30-min postdose period, an algorithm was used to identify the 30 most stable beats, as measured by the beat period, within the last 5 min of the recording, and these beats were used to compute AMP, FPD, and BP (Millard *et al.*, 2017). The simultaneous recording of multiple wells allowed for time-matched controls, permitting the investigation of noncompound induced perturbations.

Automated or semiautomated algorithms (specific to each MEA platform) were used to extract the electrophysiologic parameters described earlier. Each MEA platform contained 2 or more electrodes per well. FPD measurements were either (1) averaged across all electrodes in a given well to produce the well measurement, or (2) a single electrode was selected manually to represent a given well, with the FPD detection of that electrode used as the well measurement under baseline and drug-treated conditions. FPD measurements were rate corrected (FPDc) using the Fridericia correction (Fridericia, 2009); subsequently, the
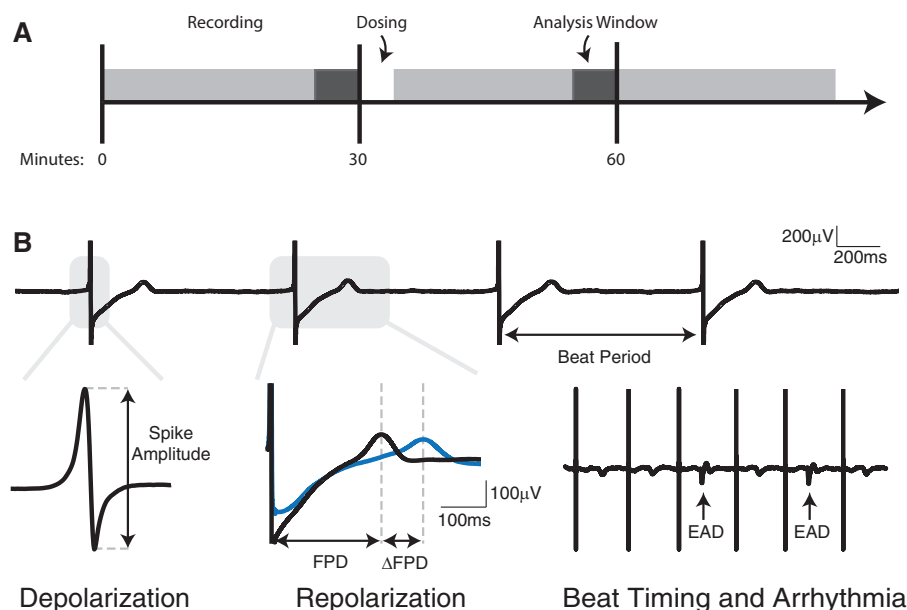
Figure 1. MEA captures 4 primary endpoints from human induced pluripotent stem cell-derived cardiomyocyte networks. A, The experimental paradigm specified 5-min recordings before and after dosing, with an equilibration period of 25 min before each recording. B, The 4 primary endpoints from the MEA assay were beat period (BP), depolarization spike amplitude (AMP), field potential duration (FPD), and the rate corrected field potential duration (FPDc). The occurrence of early after depolarizations (EADs) was also noted in subset of experiments.

percent change between the drug-treated and baseline condition was calculated for each well. Although not explicitly validated for hiPSC-CMs, the Fridericia correction is the most commonly used rate-correction formula in the in vitro cardiomyocyte literature. Raw (uncorrected) FPD values as well as FPD values corrected for changes in beating frequency are presented for direct comparison of results with previous studies.

Arrhythmia occurrence and identification of early afterdepolarization (EAD) events were marked manually through inspection of the raw field potential signal, based on previous studies that simultaneously recorded field potential and action potential signals (Asakura et al., 2015). In the field potential signal, EADs present as fast depolarization spikes that occur during (and interrupt) repolarization (Figure 1). EADs may be present in an isolated beat, in alternan patterns, or in consecutive beats. Notably, the emergence of EADs was always associated with increased variability in the beat period. Some sites and platforms used this information to implement a semiautomated algorithm for EAD detection, with manual verification of the EAD events.

Compound selection, blinding, and preparation. Eight compounds were selected for this study (Table 2). To demonstrate assay sensitivity, a set of 4 calibration compounds were used to detect block of I_{Na} (mexiletine), I_{CaL} (nifedipine), I_{Kr} (E-4031), and I_{Ks} (JNJ303). To demonstrate sensitivity to mixed ionic current blocking agents, the effects of flecainide, moxifloxacin, quinidine, and ranolazine were determined. Concentration ranges were chosen to elicit functional electrophysiologic responses based on previous reports (Braam et al., 2010; Clements and Thomas, 2014; Guo et al., 2013; Harris et al., 2013; Kitaguchi et al., 2016; Kramer et al., 2013; Navarrete et al., 2013) and known free clinical Cmax values (see Table 2). Compounds were distributed blinded by National Cancer Institute (NCI) to participating sites with instructions for preparation in DMSO, which was also provided from a common stock.

Quality control/inclusion criteria. Based on data from previously published reports (Braam et al., 2010; Clements and Thomas, 2014; Harris et al., 2013; Kitaguchi et al., 2016; Navarrete et al., 2013), studies that did not detect (1) an increase in FPDc $\geq$20% for any concentration of E-4031, and (2) a decrease in FPDc $\geq$20% for any concentration of nifedipine were excluded from the final analysis (see Supplementary Figure 1). These criteria appeared realistic for defining assay sensitivity to I_{Kr} and I_{CaL} block, respectively (2 prominent [and opposing] currents defining ventricular repolarization, an element essential to detecting effects of multiple ion channel blockade). The quality criterion was applied to an entire study (eg, mean results from cell type 1 on platform 1 at site 1), without any additional quality assessment on the single well or plate level. 10 of 18 studies fulfilled these inclusion criteria and were used in the final analysis. Results from all 18 studies are displayed in Supplementary Tables 1–3 for reference.

Statistics. A linear mixed effects model was used to quantify association between endpoints (% change of FPD, FPDc, BP, or AMP) and drug concentration (as an ordinal variable), platforms (ACA, AXN, and MCS), and cell types (AXG and CDI), according to the following equation:

End points (% change of FPD, FPDc, BP or AMP)
= Intercept
+ Fixed Effects (Platform, Cell Type, and Concentration)
+ Random Effects (Test Site) + Errors.

The analyses were performed using PROC MIXED in SAS 9.2 (SAS Institute, Cary, North Carolina). The linear mixed effects model estimation was obtained through restricted maximum likelihood. An ANOVA was also performed to determine the relative contribution of these same variables (Platform, Cell Type, Concentration) to the overall variance in the study results, both before and after administering the quality control criterion.

Table 2. Concentrations Evaluated for the 8 CiPA Pilot Study Compounds

Compound	Primary Ion Current Blocked	Free Drug (μM)	Concentrations Tested (μM)			
			1	2	3	4
Calibration compounds						
E-4031	I_{Kr}	–	0.003	0.01	0.03	0.1
Nifedipine	I_{CaL}	0.008*	0.01	0.03	0.1	0.3
Mexiletine	I_{Na}	2.503#	1	3	10	30
JNJ303	I_{Ks}	–	0.01	0.03	0.1	0.3
Test compounds						
Flecainide	I_{Kr}, I_{Na}	0.753*	0.1	0.3	1	3
Moxifloxacin	I_{Kr}, I_{CaL}	10.96*	3	10	30	100
Quinidine	I_{Kr}, I_{CaL}	3.237*	0.3	1	3	10
Ranolazine	I_{Kr}, I_{Na}	1.948#	1	3	10	30

The risk category is indicated for each compound in the CiPA compound set. "NC" is used to indicate compounds that are not categorized in the CiPA compound set. Free C_{max} values are reproduced from (*) Kramer *et al.* (2013) and (#) Crumb *et al.* (2016).
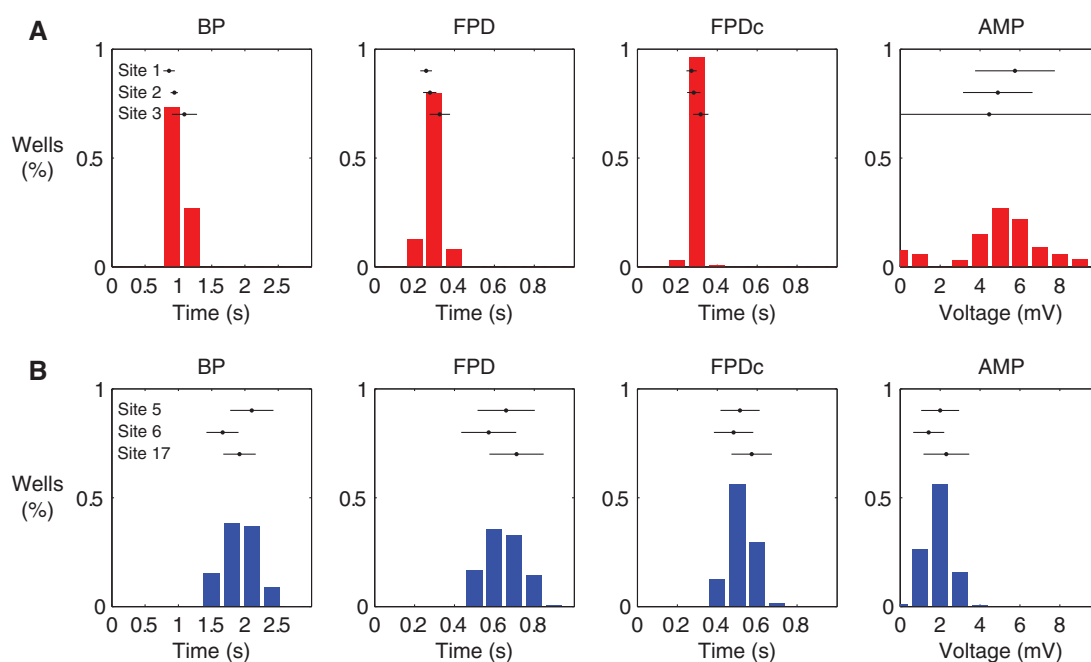

Figure 2. Baseline values of AXG and CDI cardiomyocytes across wells, plate, and sites. Each histogram summarizes data from over 300 wells for (A) AXG cells (upper) and (B) CDI cells (lower) evaluated on the AXN platform, with the mean (dot) and 95% CI (line) for each of 3 sites indicated above. The bin size is 300 ms for beat period (BP), 100 ms for field potential duration and corrected field potential duration (FPD and FPDc), and 1 mV for spike amplitude (AMP).

RESULTS

hiPSC-CMs Exhibit Stable and Reproducible Cardiac Beating

Figure 2 compares 3 primary endpoints (BP, FPD, AMP) along with derived corrected field potential (FPDc) recorded under drug-free baseline conditions across 2 cell types (CDI, lower panel, and AXG, upper panel) on the AXN MEA platform across 3 test sites. Each histogram represents over 300 wells, with endpoints included from ~100 wells per site. The mean and 95% confidence interval (CI) was computed across all wells in a study for each endpoint, and is indicated above the histogram (mean—black dot, 95% CI—horizontal error bar). For each cell type, the 95% CI's overlap, indicating a consistent electrophysiological phenotype across 3 sites for a given cell type and platform. However, the 2 cell types displayed unique electrophysiologic phenotypes in regard to BP, FPD (corrected and uncorrected), and AMP. This is not surprising given the individual manufacturing processes and proprietary media formulations. AXG myocytes (red) had a faster spontaneous beat rate and shorter FPD/FPDc as compared to CDI myocytes (blue). This observation was consistent across all 10 studies, as documented in Table 3, which contains the mean ± SD for each of the 4 endpoints across all individual studies. SCI myocytes exhibited a similar electrophysiologic phenotype to CDI myocytes. No cellular arrhythmias were observed under baseline conditions for any cell type.

hiPSC-CMs Reproduce Expected Responses to Positive and Vehicle Controls

Figure 3 shows example field potential waveforms (A–E, left) from before (black) and after (blue) exposure to the vehicle control (0.1% DMSO) and the 4 calibration compounds, along with the concentration-dependent effects on BP, FPD, FPDc, and AMP

Table 3. Average Baseline Statistics for the 4 Primary CM-MEA Assay Endpoints

| Study	Cell Type	Platform	BP (ms)	FPD (ms)	FPDc (ms)	AMP (mV)
1	AXG	AXN	861±42	258±15	271±13	5.75±1.00
2	AXG	AXN	939±27	276±17	282±17	4.89±0.87
3	AXG	AXN	1091±95	327±25	317±19	4.46±3.26
4	AXG	MCS	1042±118	346±89	341±80	1.21±1.31
5	CDI	AXN	2103±164	658±73	513±50	2.01±0.47
6	CDI	AXN	1664±133	572±69	482±49	1.36±0.47
7	CDI	MCS	1733±215	658±135	546±94	3.05±1.69
8	CDI	MCS	1364±307	580±100	524±62	1.97±1.38
9	CDI	ACA	2111±128	712±72	577±98	2.30±0.95
10	SCI	AXN	1671±156	586±45	494±29	2.43±0.96

Data are listed as the mean±the SD.
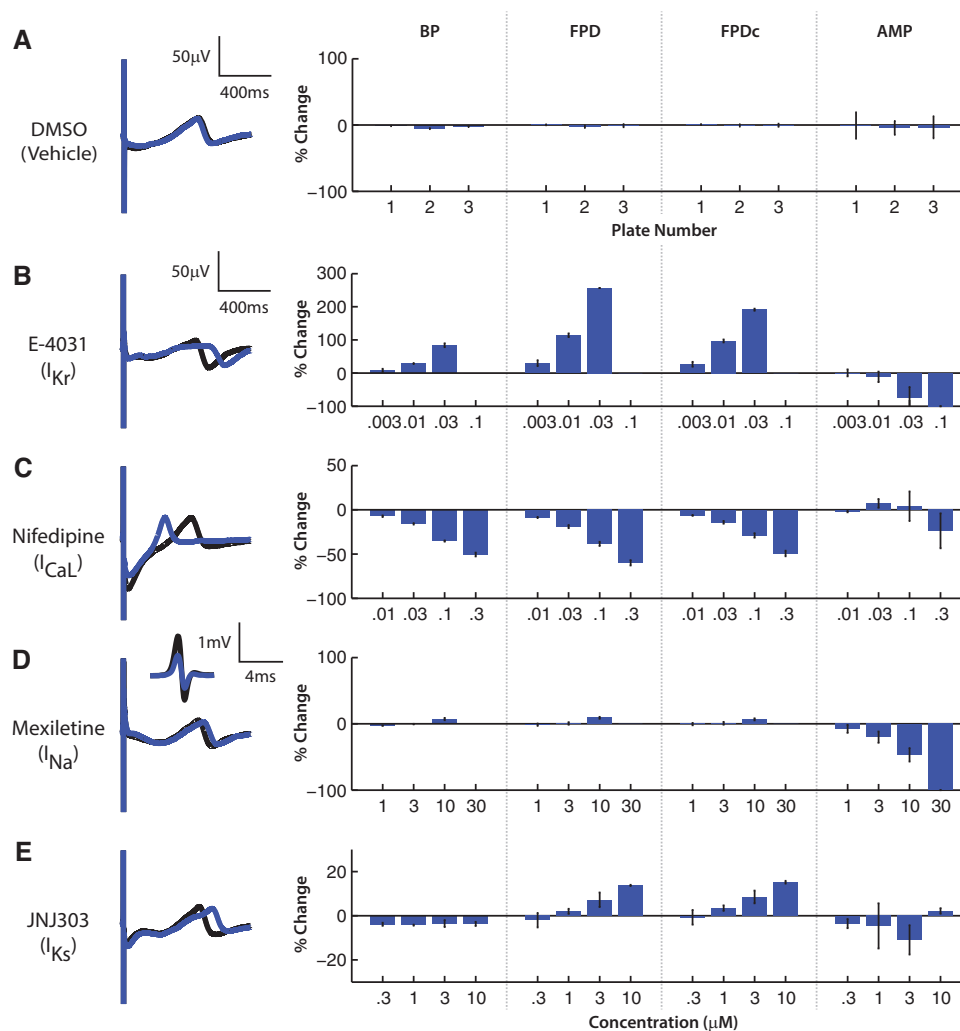
Figure 3. Control compounds demonstrate expected electrophysiological responses. Example raw field potential waveforms (left) are presented before (black) and after (blue) dosing with (A) DMSO (0.1%), (B) E-4031 (3 nM), (C) nifedipine (100 nM), (D) mexiletine (10 μM), and (E) JNJ303 (10 μM). The primary endpoints (right) are quantified across replicates at an example site (N = 3 replicates). For DMSO, each bar represents the mean across the replicates on each plate, whereas each bar represents the mean across the replicates for each concentration of the test compounds. The error bars indicate ±1 SD across the replicates. (For interpretation of the references to color in this figure legend, the reader is referred to the web version of this article.)

(A–E, right) from a single study using CDI myocytes. In this example study, the vehicle control did not produce a discernable effect across wells within a plate (N = 4), nor across plates (N = 3).

E-4031, a potent blocker of the prominent repolarizing current I_{Kr}, elicited concentration-dependent prolongation of BP, FPD, and FPDc, concentration-dependent decreases in AMP until cessation of beating at the highest concentration tested
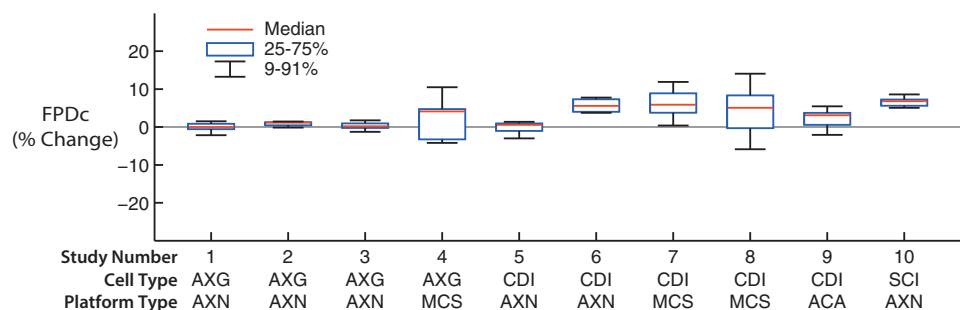
Figure 4. Vehicle controls demonstrate stable and reliable activity with CiPA core protocol. Box and whisker plots are included for each of the 10 qualified studies. The red line represents the median, the blue box marks the interquartile range, and the error bars indicate the 9%–91% range. (For interpretation of the references to color in this figure legend, the reader is referred to the web version of this article.)

(100 nM). In contrast, the L-type calcium current (I_{CaL}) blocking drug nifedipine produced concentration-dependent reductions of the beat period and shortening of FPD and FPDc, with minimal effects on AMP. For both E-4031 and nifedipine, delayed repolarization was observed before and after adjustment for the slowed (E-4031) or accelerated (Nifedipine) spontaneous pacing rate.

Mexiletine primarily blocks I_{Na} concentrations used in this study, with $I_{Ca, L}$ and I_{Kr} reduced to lesser degrees (Blinova *et al.*, 2017). As expected, mexiletine produced a concentration-dependent decrease in AMP, with minimal effects on BP, FPD, and FPDc at the highest concentrations prior to cessation of electrical activity.

JNJ303, a specific blocker of the repolarizing current I_{Ks}, only affected FPD and FPDc, displaying a consistent and small prolongation (~10%, note expanded y axis, Figure 3E) at the highest concentration tested (300 nM), which is ~5 times higher than its IC_{50} value for block of I_{Ks} and ~4 times lower than its IC_{50} value for the I_{Kr}/hERG current block (Towart *et al.*, 2009).

Inclusion Criteria Defined by Assay Sensitivity Improved Site-to-Site Reliability

The 4 positive control compounds (selected based on selectivity of current blockade) were employed to calibrate assay sensitivity and the ability of the MEA platforms to detect different drug effects. As such, inclusion criteria were implemented using the responses to E-4031 and nifedipine, requiring detection of a 20% change in FPDc for E-4031 and nifedipine (at any concentration) for data from a given study to be incorporated in the final analysis (see Methods). 10 of the 18 studies (7 sites, 3 hiPSC-CM cell types, 3 MEA platforms) satisfied the inclusion criterion and are summarized in the subsequent sections. Data from all 18 studies are provided in the Supplementary Tables and Figures for reference.

An ANOVA model was used to evaluate the contribution of compound concentration, cell type, platform, and test site to the overall variance in the study. This analysis was performed for all studies, as well as for qualified studies satisfying the inclusion criteria. The results of the ANOVA are summarized in Supplementary Table 2. In both cases, compound concentration explained the majority of the variance in the study, which was expected given concentration was driving the electrophysiological response. Prior to applying the inclusion criteria, concentration was responsible for the most variance, followed by platform type, test site, and cell type (77% of MSE vs 13%, 6%, and 4%, respectively). For the qualified study set, concentration remained responsible for the most variance, followed by comparable contributions from platform type and cell type, with

minimal contribution from test site (82% of MSE vs 9%, 8%, and 1%, respectively). Thus, applying inclusion criteria based on pharmacologic sensitivity reduced the contribution of test site variability in analysis of drug responses.

The hSC-CM-MEA Assay Produced Expected Effects on Repolarization in Qualified Studies

The percent change in FPDc after exposure to the vehicle control is presented in Figure 4 for the 10 qualified studies. The box and whisker plot indicates the median, interquartile range, and extended range for each study. None of the studies exhibited a median change in FPDc >10% for the vehicle control, which is consistent with other MEA-based studies (Ando *et al.*, 2017; Clements and Thomas, 2014). Studies 4, 7, and 8 were performed on a low well count MEA platform and exhibited greater variability in FPDc across vehicle control wells compared to other studies.

The FPDc results for the 4 calibration and 4 test compounds for all 10 qualified studies are displayed in Figure 5, with the minimal concentration at which a 20% change in FPDc was detected presented in Table 4. All wells, including those presenting EADs, were included in calculating the average %ΔFPDc (open symbols indicate at least 1 replicate exhibited EADs). E-4031 (FPDc20: median = 3 nM, span = 1 log unit) elicited prominent prolongation of repolarization for all cell types and nifedipine (FPDc20: median = 100 nM, span = 0.5 log unit) consistently exhibited repolarization shortening. The final 2 calibration compounds, mexiletine and JNJ303, produced modest and minimal prolongation of repolarization, respectively. FPDc20 was detected for mexiletine (FPDc20: median = 30 μM, span = 0.5 log unit) in 3 of 8 studies. Although the FPDc20 threshold was not attained for JNJ303, all studies did exceed ≥ 9% ΔFPDc.

The majority of studies demonstrated concentration-dependent prolongation of repolarization for each of the 4 test compounds (ranolazine, quinidine, flecainide, moxifloxacin). FPDc20 was detected for the remaining 4 test compounds in all qualified studies with 3 exceptions: beating arrested in response to flecainide addition before reaching a 20% change in FPDc in study 3 and a 20% change in FPDc was not detected for ranolazine in studies 4 and 8. Flecainide (FPDc20: median = 1 μM, span = 0.5 log unit), moxifloxacin (FPDc20: median = 100 μM, span = 0.5 log unit), quinidine (FPDc20: median = 1 μM, span = 1 log units), and ranolazine (FPDc20: median = 10 μM, span = 0.5 log unit) each consistently produced concentration-dependent prolongation of repolarization. For those drugs demonstrating prominent repolarization delays at greater concentrations, the appearance of repolarization abnormalities (consistent with early afterdepolarizations) likely contributed to the greater variability of
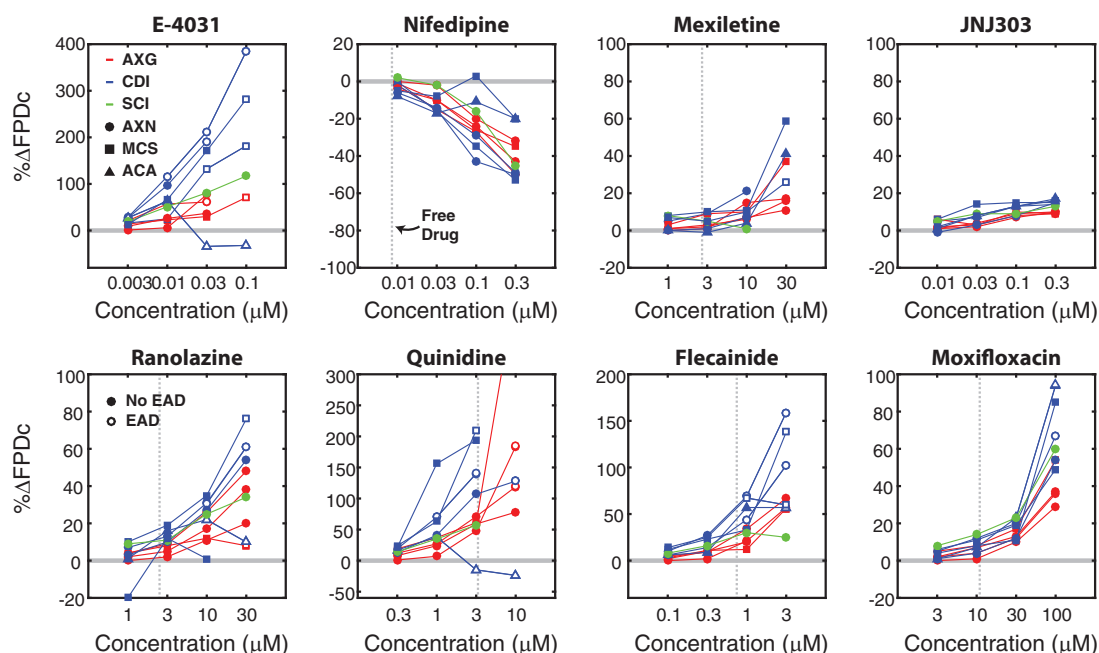
Figure 5. CM-MEA assay results display consistent trends across qualified sites and cell types. Dose response curves for FPDc (% change from baseline) are presented for each qualified study and each compound. Each point in the dose response relationship is the mean across replicates ($N{\geq}3$ replicates), including replicates exhibiting EADs, for a given compound and concentration from a single study. An open symbol indicates that EADs were detected in at least 1 replicate for that compound, concentration, and study, whereas the color and shape of the symbol indicate the cell type and platform type, respectively. The dashed gray line marks the free drug concentration listed in Table 2 for each compound.

Table 4. FPDc20 Concentrations across Each Compound and Study

| Study	Cell Type	Platform	E-4031	Nifedipine*	Mexiletine	JNJ303	Flecainide	Moxifloxacin	Quinidine	Ranolazine
1	AXG	AXN	0.03	0.3		–	1	100	3	30
2	AXG	AXN	0.003	0.1		–	1	100	1	10
3	AXG	AXN	0.01	0.1		–	Arrested	100	1	30
4	AXG	MCS	0.01	0.1	30	–	3	100	1	
5	CDI	AXN	0.003	0.1		–	1	100	1	10
6	CDI	AXN	0.003	0.1	10	–	0.3	30	1	10
7	CDI	MCS	0.01	0.1	30	–	0.3	100	0.3	10
8	CDI	MCS	0.01	0.3	30	–	0.3	100	0.3	
9	CDI	ACA	0.003	0.3	30	–	1	30	1	10
10	SCI	AXN	0.01	0.3		–	1	30	1	10

X, Did not report; *, Concentration for 20% decrease in FPDc is reported for Nifedipine. The FPDc20 is defined as the lowest concentration at which a 20% change or greater was observed in the mean across replicates for FPDc. For Nifedipine (*), the FPDc20 represents the concentration at which a 20% decrease in FPDc was detected, whereas the FPDc20 represents a 20% increase in FPDc for all other compounds. Green shading indicates all studies reporting the median FPDc20, whereas yellow shading indicates a one-half log difference from the median and white shading marks conditions where FPDc20 was not observed. FPDc20 was detected within one-half log unit of the median in all cases. JNJ303 (gray shading) consistently produced a <20% prolongation in FPDc across studies. The cells stopped beating (Arrested) in response to Flecainide in study 3. (For interpretation of the references to color in this table legend, the reader is referred to the web version of this article.)

responses observed (including, eg, the biphasic repolarization response with E-4031 and quinidine at specific sites and platforms).

Figure 6 presents the mean and SE of the concentration parameter (left) and the coefficients for the concentration, platform, and cell type parameters (table, right) for BP, AMP, FPD, and FPDc in the mixed effects model (see Methods). The coefficients for the fixed effects associated with the platform, "ACA" and "AXN" in Figure 6 correspond to the deviation of the ACA and AXN platforms relative to MCS, such that a positive value for "ACA" indicates a greater response detected on the ACA platform as compared to the MCS platform for a given compound. Similarly, the coefficient for the fixed effect associated

with the cell type, "Cell Type" in Figure 6, corresponds to the deviation of the AXG myocytes relative to the CDI myocytes, such that a negative value indicates a lower response for the AXG myocytes as compared to the CDI myocytes.

The FPDc concentration parameter was statistically significant for each of the 8 compounds (*p* value < .001, left panel of Figure 6D), with nifedipine exhibiting a negative slope (faster repolarization with increasing concentration) and the remaining 7 compounds exhibiting a positive slope (slower repolarization with increasing concentration) of varying degree. The slope in BP and FPD was also significant for all compounds, whereas the slope in AMP was significant for all compounds except JNJ303 and nifedipine.

A — %ΔBP / half-log
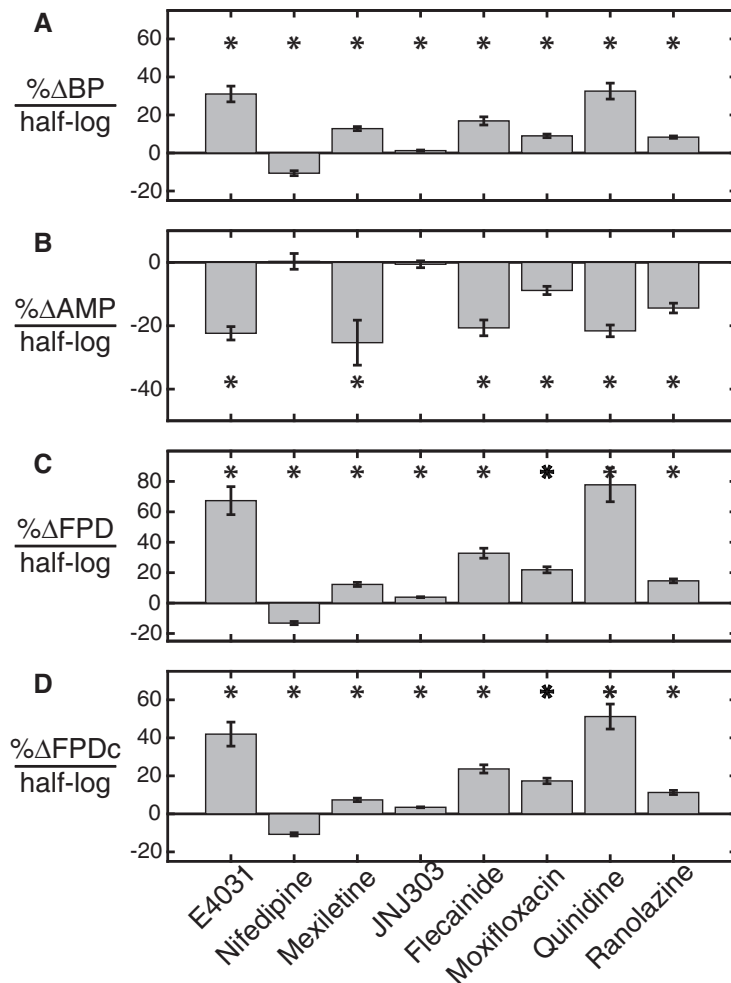
BP			
Compound	ACA	AXN	AXG	Conc.
---	---	---	---	---
E-4031	-4.6	0.1	-80.8	31.0
Nifedipine	-12.5	-5.8	12.0	-10.6
Mexiletine	-22.9	-12.0	-1.9	12.8
JNJ303	-10.6	-1.6	-3.0	1.2
Flecainide	-22.9	-7.0	-8.0	16.9
Moxifloxacin	-0.9	-4.0	-6.6	9.0
Quinidine	-41.7	-63.3	-4.8	32.5
Ranolazine	-4.6	-3.2	-1.2	8.3

B — %ΔAMP / half-log

AMP			
Compound	ACA	AXN	AXG	Conc.
---	---	---	---	---
E-4031	-5.0	-7.9	-18.4	-22.4
Nifedipine	33.6	4.2	5.5	0.3
Mexiletine	-22.2	-28.5	-6.9	-25.3
JNJ303	3.2	5.1	-1.3	-0.6
Flecainide	-5.1	-5.8	-6.5	-20.7
Moxifloxacin	1.1	-11.3	0.1	-8.9
Quinidine	-4.5	-18.9	-15.0	-21.6
Ranolazine	8.5	-11.4	-12.2	-14.4

C — %ΔFPD / half-log

FPD			
Compound	ACA	AXN	AXG	Conc.
---	---	---	---	---
E-4031	-102.7	73.0	-119.8	67.4
Nifedipine	-1.0	-5.5	8.2	-13.2
Mexiletine	-17.5	-10.3	-7.3	12.3
JNJ303	-4.5	-2.2	-5.3	3.9
Flecainide	-24.9	-3.5	-28.1	32.8
Moxifloxacin	5.7	-8.0	-10.7	21.9
Quinidine	-192.6	-118.7	-12.2	77.8
Ranolazine	-10.1	2.7	-16.7	14.6

D — %ΔFPDc / half-log

FPDc			
Compound	ACA	AXN	AXG	Conc.
---	---	---	---	---
E-4031	-80.4	50.9	-75.6	41.9
Nifedipine	4.9	-4.4	5.4	-10.8
Mexiletine	-9.0	-5.6	-6.1	7.3
JNJ303	-0.4	-1.7	-3.9	3.5
Flecainide	-13.0	0.4	-23.2	23.6
Moxifloxacin	4.6	-5.9	-7.5	17.3
Quinidine	-135.4	-63.3	-16.8	51.2
Ranolazine	-7.1	4.1	-15.0	11.3

Bold p<0.05
p<0.001

Figure 6. CM-MEA assay detected a concentration-dependent repolarization effects for each compound. Left panel. A linear mixed effects model established that each compound produced a significant dose-dependent change in FPDc (* marks $p < .001$). The results for each of the 10 studies were used to fit the mixed effects model. The concentration parameter from the mixed effects model is plotted (left) for (A) BP, (B) AMP, (C) FPD, and (D) FPDc, whereas model parameters for fixed effects associated with platform, cell type, and concentration are detailed in the tables (right). In the tables, the bold typeface indicates $p < .05$ and the yellow background indicates $p < .001$. (For interpretation of the references to color in this figure legend, the reader is referred to the web version of this article.)

FPDc responses were less in magnitude with AXG than with CDI cells for all compounds. Indeed, for 7 of the 8 compounds (quinidine as the exception), the cell type was a significant effect for FPDc (p value $< .05$). Again, this agrees with the qualitative observation that CDI myocytes demonstrated a greater change in FPDc in response to the majority of compounds. The platform type was only significant for 4 of 8 compounds for FPDc (p value $< .05$).

The incidence of EAD-like activity for all compounds is summarized in Table 5. E-4031 and quinidine consistently exhibited EADs across all cell types and studies, whereas EADs were detected more frequently for CDI cells for flecainide and moxifloxacin at targeted drug concentrations greater than C_{max}. No EADs were reported for nifedipine or JNJ303 across all studies, and were thus excluded from the table.

Cross-Platform Comparisons Across a Single Operator Indicate Consistency of the CM-MEA Assay

A single site performed 4 studies across 2 platforms (AXN and MCS) and 2 cell types (AXG myocytes, Figs. 7A and C; CDI myocytes, Figs. 7B and D) with all 8 compounds, thus enabling a comparison of FPDc responses across 2 platforms and myocytes

for the same operator. For each cell type, the percent change in FPDc for the AXN platform (horizontal axis) was correlated with the percent change in FPDc for the MCS platform (vertical axis). Each data point represents the mean response for FPDc across replicates at a single concentration for a single drug ($N = 32$ points). Data points were excluded from the graph if beating had arrested or if one or more replicates exhibited EADs. The change in FPDc was correlated across the 2 MEA platforms for each cell type, as illustrated by the proximity of the data to the unity line (black) and the correlation coefficients (AXG: $R = 0.88$; CDI: $R = 0.97$).

Bland-Altman analysis was also performed for each cell type (AXG: Figure 7C; CDI: Figure 7D) to quantitatively determine the bias and limits of agreement between the assays performed on the 2 platform types (Bland and Altman, 1986). This analysis contrasts the differences between the %ΔFPDc measured for the 2 platforms (at each compound and concentration) with the average values from the 2 platforms. The mean difference, termed the bias (solid line), was not significant for either cell type (CDI: Bias = 0.50, 95% CI = [−1.84 2.84]; AXG: Bias = 0.48, 95% CI = [−3.93 4.89]). The limits of agreement (LOA, dashed lines) mark the range of differences between the 2 platforms that are

Table 5. EAD Occurrence Reported across Individual Studies

Study	Cell Type	Platform	E-4031 0.003	E-4031 0.01	E-4031 0.03	E-4031 0.1	Mexiletine 1	Mexiletine 3	Mexiletine 10	Mexiletine 30	Flecainide 0.1	Flecainide 0.3	Flecainide 1	Flecainide 3	Moxifloxacin 3	Moxifloxacin 10	Moxifloxacin 30	Moxifloxacin 100	Quinidine 0.3	Quinidine 1	Quinidine 3	Quinidine 10	Ranolazine 1	Ranolazine 3	Ranolazine 10	Ranolazine 30
1	AXG	AXN																				3/3				
2	AXG	AXN			2/3	2/3																2/3				
3	AXG	AXN																								
4	AXG	MCS				3/4								1/3								3/3				3/4
5	CDI	AXN			1/4	2/4							2/4	1/4								2/3				
6	CDI	AXN		3/3	3/3	3/3							1/3	1/3				3/3		3/3	3/3	Q			3/3	3/3
7	CDI	MCS			3/3	3/3								3/3							1/3	3/3				3/3
8	CDI	MCS								3/3			6/7	4/4								4/4				5/5
9	CDI	ACA	1/3	3/3	3/3	3/3								3/3			1/3	2/3		1/3	3/3	2/3			3/3	2/3
10	SCI	AXN		2/3	2/3	3/3				Q			1/3	2/3			1/3	2/3		2/3	3/3	Q			1/3	2/3

EAD occurrence is reported as a proportion of replicates exhibiting EADs for each compound and concentration. JNJ303 and nifedipine were omitted from the table as none of the studies reported EADs at any concentration for these compounds. The concentrations are listed in μM.
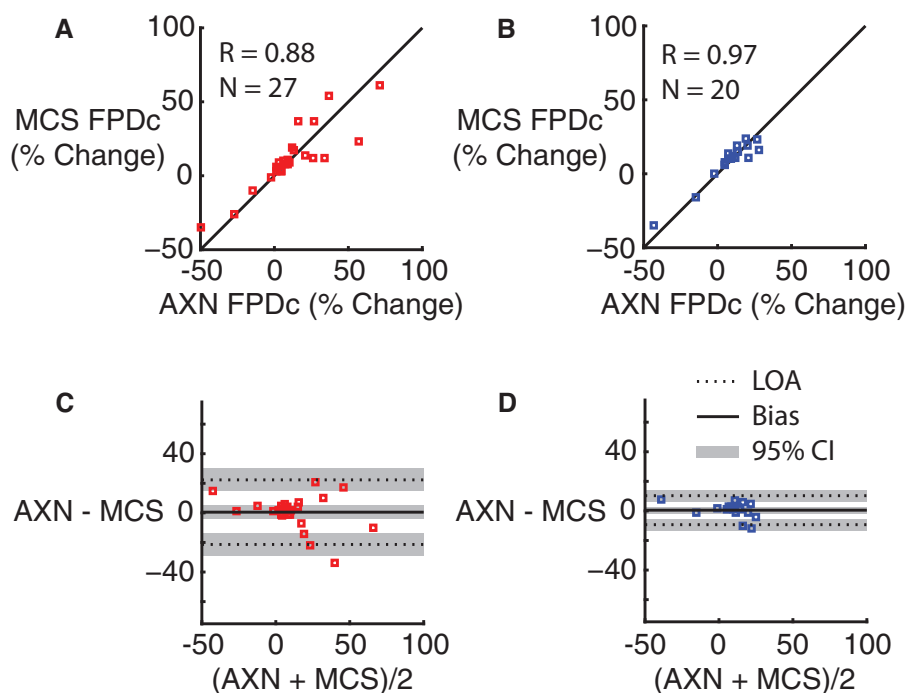
Figure 7. CM-MEA results are correlated across distinct platforms evaluated by a single operator. The FPDc (% change from baseline) results from a single site are compared across 2 MEA platforms. The top left panel (A) shows the results with AXG cells, whereas the top right panel (B) presents the results from the CDI cells. Each data point represents the mean across replicates for a given compound and concentration evaluated on each platform. (C) and (D) present Bland-Altman plots for AXG and CDI cells, respectively. In each plot, the difference in %ΔFPDc across the 2 platforms is compared to the mean across the 2 platforms, with each point representing a single compound and concentration. The bias (solid line) and limits of agreement (dashed line) derived from the data are included, along with the 95% CIs (gray shaded region).

expected for 95% of measurements (CDI: LOA = [−9.3 10.3]; AXG: LOA = [−21.36 22.32]). By comparison, if EADs were included, the limits of agreement were much larger (CDI: Bias = −11.90, LOA = [−100.60 to 76.79]; AXG: Bias = 8.00, LOA = [−107.60 123.60]), suggesting that absolute changes in %ΔFPDc are less reliable across measurements when repolarization irregularities, such as EADs, occur.

DISCUSSION

A common protocol was utilized across 3 MEA platforms, 4 hSC-CM cell types, and 18 individual studies with blinded analysis to evaluate the suitability of a CM-MEA assay for cardiac safety testing. Inclusion criteria based on delayed repolarization with block of the repolarizing hERG (I_{Kr}) current and shortened repolarization with block of the depolarizing L-type calcium current were applied to serve as appropriate experimental controls and verify functional ionic currents in the hiPSC-CMs and analysis approaches for the MEA platforms. 10 of the 18 studies (7 sites, 3 hiPSC-CM cell types, 3 MEA platforms) satisfied the inclusion criterion and exhibited consistent concentration-response curves for the 8 drugs tested (4 chosen to test for functional I_{Kr}, I_{Ks}, I_{CaL}, and I_{Na}, and another 4 chosen to represent mixed ion current blockers).

For the qualified studies (demonstrating FPDc prolongation with E-4031 and FPDc shortening with nifedipine), each of the 6 remaining compounds elicited significant and reliable responses from the 4 primary MEA endpoints, thus confirming assay sensitivity to selective ion channel block and multichannel block. E-4031, a potent I_{Kr} blocker, produced significant prolongation of BP, FPD, and FPDc, while nifedipine, an I_{CaL} blocker, shortened BP, FPD, and FPDc, consistent with published

experimental reports (Braam et al., 2010; Clements and Thomas, 2014; Harris et al., 2013; Kitaguchi et al., 2016; Navarrete et al., 2013). Mexiletine, an I_{Na} blocker, elicited a significant reduction in AMP, with only subtle changes in repolarization. JNJ303, an I_{Ks} blocker, consistently produced concentration-dependent prolongation of FPDc across sites. Multisite detection of subtle, yet significant, changes in repolarization to JNJ303 are consistent with some reports (Clements and Thomas, 2014; Kitaguchi et al., 2016) and contrary to others (Qu and Vargas, 2015), but highlight the sensitivity of the CM-MEA assay and may suggest a contributing role of I_{Ks} current to the hSC-CM action potential (Braam et al., 2013).

The 4 mixed ionic current blocking drugs (ranolazine, quinidine, flecainide, and moxifloxacin) all exhibit I_{Kr} block along with additional multiion channel block in the range of concentrations tested (Blinova et al., 2017; Crumb et al., 2016; Kramer et al., 2013). In this report, each of these compounds produced qualitatively similar responses, with prolongation of BP, FPD, and FPDc, and reduction in AMP, consistent with previously published reports (Blinova et al., 2017; Braam et al., 2010; Clements and Thomas, 2014). Each of these multiion channel blockers also produced EAD-like activity in at least one cell type at the highest concentration tested. In addition to the dose response trends, study-to-study comparisons were defined using FPDc20, defined as the concentration at which a 20% change in FPDc was detected for each compound. Even when combined across cell types, the FPDc20 detected was within a half log deviation from the median across studies for each of the compounds. The only exception was that studies 4 and 8 did not detect a 20% change in FPDc for ranolazine at any of the concentrations. FPDc20 for mexiletine, which produced only modest prolongation of FPDc, was observed in half of the studies,

whereas FPDc20 was not observed for JNJ303 in any of the studies.

About 8 of 18 studies (44%) failed to detect delayed repolarization with the I_{Kr} blocking drug E-4031 and shortened repolarization with the L-type calcium channel blocker nifedipine. Such low study sensitivity could result from inadequate drug exposures, poor culture techniques, differences in ion channel densities, improper environmental controls, or analysis techniques not accurately capturing electrophysiologic responses. The inclusion criterion utilized in this report (minimum 20% change in repolarization for any dose of both drugs) is not a specific recommendation for quality assessment moving forward, but rather exemplary of the need for a standardized approach for evaluating assay sensitivity. Calibration of systems with well-characterized reference standards will be critical to facilitate risk assessment and ranking of compound liabilities for internal pharmaceutical decisions as well as regulatory reviews of nonclinical data.

FPDc20 was used as a threshold to demonstrate assay sensitivity and assess reproducibility across cell types and experiment sites. However, use in this context should not be taken as a validation of its adoption for pro-arrhythmic risk as there are several shortcomings in the measurement. As a threshold-based computation, there is an inherent trade-off between assay sensitivity and specificity, particularly when considering differences across cell types and platforms. Further, FPDc20 does not explicitly account for the differences in drug sensitivity across commercial cell types described here, as the relevant parameters and associated thresholds that define significance may be specific to each cell type.

A subset of experiments allowed a direct comparison across 2 MEA platforms and 2 commercial hiPSC-CM cell types from the same site and operator. Although a high correlation for the 2 MEA platforms was found for both cell types, there were also clear, if not expected, deviations in the electrophysiologic responses across the 2 cell types. In general, CDI myocytes exhibited a greater sensitivity to repolarization effects with each of the 8 compounds, and a higher propensity for generating EADs. This difference could be related to the slower spontaneous beating rate and/or FPDc of CDI myocytes at baseline. The Fridericia rate correction attempts to remove the influence of beat rate on FPD, but has not been explicitly validated for hiPSC-CMs and is likely different with different cell types (Hortigon-Vinagre et al., 2016; Rast et al., 2016). In addition, simple rate-correction calculations do not account for reverse use-dependence (Shah and Hondeghem, 2005), a phenomenon describing the increased prolongation of repolarization at slow beating rates. This observation should be considered in future assay guidelines, in that results could differ based on the hSC-CM specific changes in beat rate elicited by drugs. In this study, drugs that delayed repolarization also slowed spontaneous beating (prolonging beat period), although the effect on repolarization was less when using corrected (vs uncorrected) FPD measures. The qualitative link between delayed repolarization and slower beating rates may reflect: (1) delays in returning to diastolic potentials (due to prolongation of the action potential duration) leading to delays in resetting of pacemaker mechanisms (responsible for diastolic depolarization) and slower pacing, or (2) greater repolarization delays observed at slower stimulation rates in the presence of I_{Kr} block (termed reverse-use-dependence), or other mechanisms. Utilization of a paced cardiomyocyte assay, whereby the beat rate is controlled through electrical or optogenetic stimulation, would eliminate variability due to changes in spontaneous beating across cell types (especially myocytes displaying slow intrinsic beating rates).

Despite inherent electrophysiologic differences across the MEA platforms and commercial cell types, these pilot study results demonstrate that consistent concentration-dependent effects on repolarization can be achieved across multiple study sites and platforms using standardized protocols and data inclusion criteria, in agreement with other recent reports (Blinova et al., 2017; Kitaguchi et al., 2016). A linear mixed effects model revealed that, (1) qualifying test sites based on assay sensitivity to pharmacological block of I_{Kr} and I_{CaL} reduced variability attributed to test sites, (2) cell type did affect the extent of delayed repolarization for most drugs, and (3) drug concentration had the most significant effect on delaying repolarization, with a statistically significant relationship observed between concentration and FPDc for each of the 8 compounds. An ongoing CiPA validation study will build upon the core protocol from this pilot study to further establish intersite reliability, systemic limitations, and risk assessment by testing a significantly larger (28) compound set representing drugs with high, intermediate, and low/no levels of proarrhythmic risk based on clinical findings. The results reported here support that effort, and the utility of hiPSC-CM assays for cardiac safety evaluation.

SUPPLEMENTARY DATA

Supplementary data are available at *Toxicological Sciences* online.

DISCLOSURES

FUNDING

ACKNOWLEDGMENTS

at Stanford Cardiovascular Institute for testing of drug compounds on SCI hSC-CM line. The content of this publication does not necessarily reflect the views or policies of the Department of Health and Human Services, nor does mention of trade names, commercial products, or organizations imply endorsement by the U.S. Government.

REFERENCES

Ando, H., Yoshinaga, T., Yamamoto, W., Asakura, K., Uda, T., Taniguchi, T., Ojima, A., Shinkyo, R., Kikuchi, K., Osada, T., et al. (2017). A new paradigm for drug-induced torsadogenic risk assessment using human iPS cell-derived cardiomyocytes. *J. Pharmacol. Toxicol. Methods* **84**, 111–127.

Asai, Y., Tada, M., G. Otsuji, T., and Nakatsuji, N. (2010). Combination of functional cardiomyocytes derived from human stem cells and a highly-efficient microelectrode array system: An ideal hybrid model assay for drug development. *Curr. Stem Cell Res. Ther.* **5**, 227–232.

Asakura, K., Hayashi, S., Ojima, A., Taniguchi, T., Miyamoto, N., Nakamori, C., Nagasawa, C., Kitamura, T., Osada, T., Honda, Y., et al. (2015). Improvement of acquisition and analysis methods in multi-electrode array experiments with iPS cell-derived cardiomyocytes. *J. Pharmacol. Toxicol. Methods.* **75**, 17–26.

Bland, J. M., and Altman, D. G. (1986). Statistical methods for assessing agreement between two methods of clinical measurement. *Lancet (London, England)* **327**, 307–310.

Blinova, K., Stohlman, J., Vicente, J., Chan, D., Johannesen, L., Hortigon-Vinagre, M. P., Zamora, V., Smith, G., Crumb, W. J., Pang, L., et al. (2017). Comprehensive translational assessment of human-induced pluripotent stem cell derived cardiomyocytes for evaluating drug-induced arrhythmias. *Toxicol. Sci.* **155**, 234–247.

Braam, S. R., Tertoolen, L., Casini, S., Matsa, E., Lu, H. R., Teisman, A., Passier, R., Denning, C., Gallacher, D. J., Towart, R., et al. (2013). Repolarization reserve determines drug responses in human pluripotent stem cell derived cardiomyocytes. *Stem Cell Res.* **10**, 48–56.

Braam, S. R., Tertoolen, L., van de Stolpe, A., Meyer, T., Passier, R., and Mummery, C. L. (2010). Prediction of drug-induced cardiotoxicity using human embryonic stem cell-derived cardiomyocytes. *Stem Cell Res.* **4**, 107–116.

Clements, M., and Thomas, N. (2014). High-throughput multi-parameter profiling of electrophysiological drug effects in human embryonic stem cell derived cardiomyocytes using multi-electrode arrays. *Toxicol. Sci.* **140**(2), 445–461.

Crumb, W. J., Vicente, J., Johannesen, L., and Strauss, D. G. (2016). An evaluation of 30 clinical drugs against the comprehensive in vitro proarrhythmia assay (CiPA) proposed ion channel panel. *J. Pharmacol. Toxicol. Methods.* **81**, 251–262.

Fridericia, L. S. (2003). The Duration of Systole in an Electrocardiogram in Normal Humans and in Patients with Heart Disease. *Acta Med. Scand.* **8**, 343–351.

Guo, L., Coyle, L., Abrams, R. M. C., Kemper, R., Chiao, E. T., and Kolaja, K. L. (2013). Refining the human iPSC-cardiomyocyte arrhythmic risk assessment model. *Toxicol Sci.* **136**(2), 581–594.

Gintant, G., Sager, P. T., and Stockbridge, N. (2016). Evolution of strategies to improve preclinical cardiac safety testing. *Nat. Rev. Drug Discov.* **15**, 457–471.

Harris, K., Aylott, M., Cui, Y., Louttit, J. B., McMahon, N. C., and Sridhar, A. (2013). Comparison of electrophysiological data from human-induced pluripotent stem cell-derived cardiomyocytes to functional preclinical safety assays. *Toxicol. Sci.* **134**, 412–426.

Hortigon-Vinagre, M. P., Zamora, V., Burton, F. L., Green, J., Gintant, G. A., and Smith, G. L. (2016). The use of ratiometric fluorescence measurements of the voltage sensitive dye Di-4-ANEPPS to examine action potential characteristics and drug effects on human induced pluripotent stem cell-derived cardiomyocytes. *Toxicol. Sci.* **154**(2), 320–331.

Johannesen, L., Vicente, J., Mason, J. W., Sanabria, C., Waite-Labott, K., Hong, M., Guo, P., Lin, J., Sørensen, J. S., Galeotti, L., et al. (2014). Differentiating drug-induced multichannel block on the electrocardiogram: Randomized study of dofetilide, quinidine, ranolazine, and verapamil. *Clin. Pharmacol. Ther.* **96**, 549–558.

Kitaguchi, T., Moriyama, Y., Taniguchi, T., Ojima, A., Ando, H., Uda, T., Otabe, K., Oguchi, M., Shimizu, S., Saito, H., et al. (2016). CSAHi study: Evaluation of multi-electrode array in combination with human iPS cell-derived cardiomyocytes to predict drug-induced QT prolongation and arrhythmia–effects of 7 reference compounds at 10 facilities. *J. Pharmacol. Toxicol. Methods* **78**, 93–102.

Kramer, J., Obejero-Paz, C. A., Myatt, G., Kuryshev, Y. A., Bruening-Wright, A., Verducci, J. S., and Brown, A. M. (2013). MICE models: Superior to the HERG model in predicting Torsade de Pointes. *Sci. Rep.* **3**, 2100.

Ma, J., Guo, L., Fiene, S. J., Anson, B. D., Thomson, J. A., Kamp, T. J., Kolaja, K. L., Swanson, B. J., and January, C. T. (2011). High purity human-induced pluripotent stem cell-derived cardiomyocytes: Electrophysiological properties of action potentials and ionic currents. *Am. J. Physiol. Heart Circ. Physiol.* **301**, H2006–H2017.

Meiry, G., Reisner, Y., Feld, Y, Goldberg, S, Rosen, M, Ziv, N, and Binah, O. (2001). Evolution of action potential propagation and repolarization in cultured neonatal rat ventricular myocytes. *J. Cardiovasc. Electrophysiol.* **12**, 1269–1277.

Millard, D.C., Clements, M., Ross, J.D. (2017). The CiPA Microelectrode Array Assay with hSC-Derived Cardiomyocytes: Current Protocol, Future Potential. In: Clements, M., Roquemore, L. (eds) Stem Cell-Derived Models in Toxicology. Methods in Pharmacology and Toxicology. Humana Press, New York, NY pp. 83–107.

Nakamura, Y., Matsuo, J., Miyamoto, N., Ojima, A., Ando, K., Kanda, Y., Sawada, K., Sugiyama, A., and Sekino, Y. (2014). Assessment of testing methods for drug-induced repolarization delay and arrhythmias in an iPS cell-derived cardiomyocyte sheet: Multi-site validation study. *J. Pharmacol. Sci.* **124**, 494–501.

Navarrete, E. G., Liang, P., Lan, F., Sanchez-Freire, V., Simmons, C., Gong, T., Sharma, A., Burridge, P. W., Patlolla, B., Lee, A. S., et al. (2013). Screening drug-induced arrhythmia events using human induced pluripotent stem cell-derived cardiomyocytes and low-impedance microelectrode arrays. *Circulation* **128**, S3–13.

Qu, Y., and Vargas, H. M. (2015) Proarrhythmia risk assessment in human induced pluripotent stem cell-derived cardiomyocytes using the maestro MEA platform. *Toxicol. Sci.* **147**(1), 286–295.

Rast, G., Kraushaar, U., Buckenmaier, S., Ittrich, C., and Guth, B. D. (2016). Influence of field potential duration on spontaneous beating rate of human induced pluripotent stem cell-derived cardiomyocytes: Implications for data analysis and test system selection. *J. Pharmacol. Toxicol. Methods* **82**, 74–82.

Reppel, M., Pillekamp, F., Lu, Z. J., Halbach, M., Brockmeier, K., Fleischmann, B. K., and Hescheler, J. (2004). Microelectrode arrays: A new tool to measure embryonic heart activity. *J. Electrocardiol.* **37**, 104–109.

Sager, P. T., Gintant, G., Turner, J. R., Pettit, S., and Stockbridge, N. (2014). Rechanneling the cardiac proarrhythmia safety paradigm: A meeting report from the Cardiac Safety Research Consortium. *Am. Heart J.* **167**, 292–300.

Shah, R. R., and Hondeghem, L. M. (2005). Refining detection of drug-induced proarrhythmia: qT interval and TRIaD. *Heart Rhythm* **2**, 758–772.

Thomas, C., Jr, Springer, P., Loeb, G., Berwaldnetter, Y., and Okun, L. (1972). A miniature microelectrode array to monitor the bioelectric activity of cultured cells. *Exp. Cell Res.* **74**, 61–66.

Towart, R., Linders, J. T. M., Hermans, A. N., Rohrbacher, J., van der Linde, H. J., Ercken, M., Cik, M., Roevens, P., Teisman, A.,

Gallacher, D. J., *et al*. (2009). Blockade of the IKspotassium channel: An overlooked cardiovascular liability in drug safety screening? *J. Pharmacol. Toxicol. Methods* **60**, 1–10.

van den Heuvel, N. H. L., van Veen, T. A. B., Lim, B., and Jonsson, M. K. B. (2014). Lessons from the heart: Mirroring electrophysiological characteristics during cardiac development to in vitro differentiation of stem cell derived cardiomyocytes. *J. Mol. Cell. Cardiol.* **67**, 12–25.